Journal of Colloid and Interface Science **209,** 154–161 (1999)
Article ID jcis.1998.5882, available online at http://www.idealibrary.com on IDEAL®

A Combined Surface-Enhanced Raman–X-Ray Photoelectron Spectroscopic Study of 2-mercaptobenzothiazole Monolayers on Polycrystalline Au and Ag Films

N. Sandhyarani,* G. Skanth,* Sheela Berchmans,† V. Yegnaraman,† and T. Pradeep*,[1]

*Department of Chemistry and Regional Sophisticated Instrumentation Centre, Indian Institute of Technology, Madras 600 036, India; and †Electrodics and Electrocatalysis Division, Central Electrochemical Research Institute, Karaikudi, Tamilnadu 630 006, India

Received May 11, 1998; accepted September 23, 1998

The monolayers of 2-mercaptobenzothiazole (MBT) on polycrystalline Au and Ag films have been studied by surface-enhanced Raman (SERS) and X-ray photoelectron (XPS) spectroscopies. Whereas MBT adsorbs with its molecular plane flat on Ag, its plane is perpendicular on Au. This difference in adsorbate geometry is manifested as differences in the intensities of certain vibrational peaks in the Raman spectra. *Ab initio* **molecular orbital (MO) calculations suggest that MBT adsorbs on Au in the thione form and on Ag in the thiol form. The monolayers are stable up to a temperature of 473 K, much higher than most of the self-assembled monolayers (SAMs) studied so far. The adsorption geometry does not undergo any significant change when the monolayers are heated, although minor changes are observed in the SER spectra of the Ag monolayer. Raman intensities of all the bands increase with heating, and the enhanced intensity is preserved even after cooling. This is attributed to monolayer-induced coalescence of gold islands leading to the formation of an extended self-assembly. XPS studies confirm chemisorption, although structural details are not manifested.** © 1999 Academic Press

Key Words: **self-assembled monolayers; surface-enhanced Raman spectroscopy;** *ab initio* **MO calculations; X-ray photoelectron spectroscopy.**

INTRODUCTION

Self-assembly of organic surfactant molecules, leading to compact monolayers, is one of the principal means of synthesizing functional molecular surfaces (1). These monolayers are formed by the specific chemical binding between the surface and the head group and the van der Waals interaction among the molecules after their initial chemisorption. Such surfaces are predicted to be useful in making chemical sensors, optoelectronic materials, and several futuristic devices (2). A variety of methodologies have been used to effect changes in the monolayers leading to functional surfaces, and reactions with low energy ions is one among them (3). We have been working along this line in the past few years, and molecular-level functionalization has been achieved by gas-phase (4) as well as solution-phase (5) processes.

While we were working with these problems, it became necessary to study various monolayers with different tools of surface science. We have established that order in alkanethiol monolayers can be probed with X-ray photoelectron spectroscopy (XPS) and a simple measure of the monolayer thickness is possible from the analysis of secondary electron background (6). Alkanethiol monolayers were also investigated by surface-enhanced Raman spectroscopy (SERS) (7). These monolayers desorb after melting to form liquid-like structures. Studies show that the kinetics of initial adsorption and that of self-organization are different, and they depend strongly on the chain length.

This study is an extension of earlier investigations and focuses on the chemisorption of 2-mercaptobenzothiazole (MBT). In an earlier investigation of 1,4-benzenedimethanethiol (BDMT), we established that chemisorption geometry is different for gold and silver (8). Whereas on Au the molecule adsorbs perpendicular to the surface with one thiol group protruding at the surface, chemisorption on Ag leads to a flat geometry. The Au monolayer, due to the preferred adsorption geometry, shows significant dynamics upon heating. These results prompted us to investigate systems where possibilities of different adsorption geometries exist. MBT is an intensely investigated system in the electrochemical context, particularly in relation to modified electrodes (9). This is due to its capacity to inhibit electrode corrosion and its relatively high stability at the surface. Adsorption of MBT on Ag surfaces has been investigated by attenuated total reflection infrared (ATR IR) spectroscopy (10). A strong Ag–S stretching frequency (10) is observed to occur at 1005 cm^{-1}. It has been suggested that the molecules adsorbing at the edges of the metal islands are the ones contributing to the IR intensity. The MBT monolayer on Au has also been the subject of electrochemical investigations (11, 12). While the Au–MBT surface allows the redox kinetics of ferro-ferricyanide to remain unhindered, it also blocks the under-potential deposition of copper and the redox behavior of the ferrous-ferric system, thereby suggesting the possibility of

[1] To whom correspondence should be addressed.

0021-9797/99 $30.00

using SAM for distinguishing between inner- and outer-sphere electron transfer reactions (12).

In the following, we present a surface-enhanced Raman spectroscopic (SERS) investigation of MBT monolayers on polycrystalline Au and Ag films. Adsorption of MBT on Ag has been the subject of three previous SERS investigations (13–15). Ohsawa and Suetaka (15) conclude that MBT adsorbs in the thiol form on Ag. A SERS study of MBT adsorption on Ag subcolloidal particles (14) suggests an adsorption geometry in which the sulfur atoms chemisorb on Ag. Adsorption of the related molecule, 2-mercaptobenzimidazole (MBI) on Au and Ag was also investigated by SERS (16). Exposure of this molecule on the surface at room temperature leads to an initial chemisorption. Whereas on Ag warming the surface leads to reaction, on Au the adsorption geometry undergoes a drastic change. Subtle differences in the Raman spectra were used to infer the structural changes. SERS of MBI adsorption on Cu was investigated by Xue and Zhang as well (17). Benzimidazole has also been investigated by inelastic electron tunneling spectroscopy (IETS) (18).

An analysis of SERS of the MBT monolayers on the basis of published SERS selection rules (19–21) conclusively establishes a near-perpendicular molecular geometry for Au and an almost parallel geometry for Ag. Variable temperature measurements definitively establish the high stability of the monolayer system—much higher than most of the monolayers studied so far. Temperature-dependent variations in geometry are minimal for both the surfaces investigated. However, monolayer-assisted annealing of the gold islands occurs, leading to the formation of a denser molecular assembly. This leads to an enhancement in the total Raman intensity upon heating and subsequent cooling. This effect is particularly noticeable on Au, whereas in Ag annealing appears to create different adsorption geometries. XPS investigations compliment the SERS data.

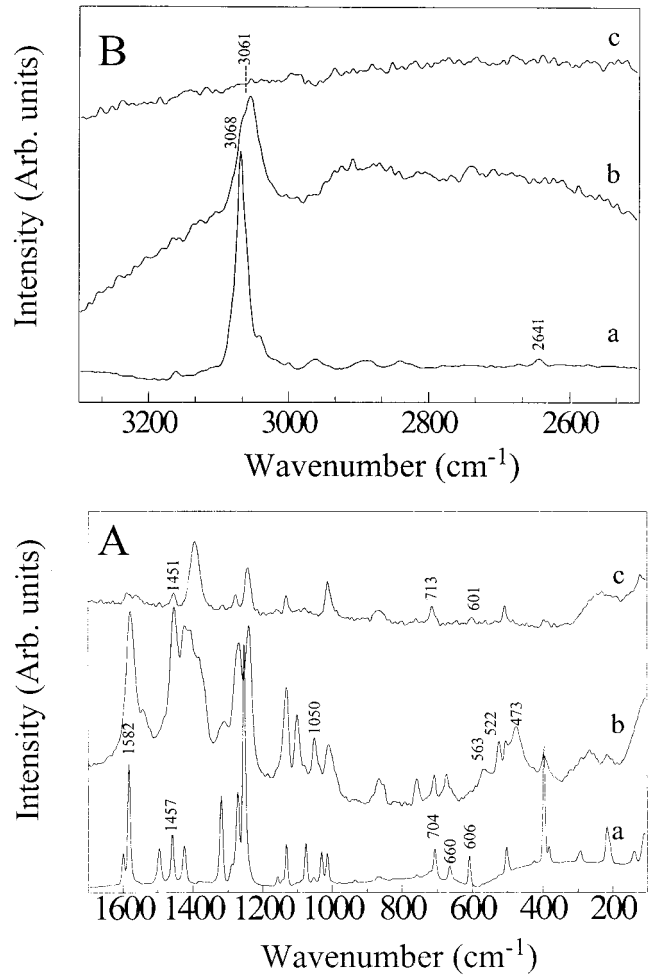

FIG. 1. (A) Normal Raman spectrum of (a) MBT solid and SER spectra of MBT monolayers on (b) Au and (c) Ag surfaces. (B) C–H regions of the above.

EXPERIMENTAL

Details of the experimental procedure for the preparation of SERS active surfaces has been described in detail earlier (22). Briefly, the methodology involves sputter coating of Au or Ag of 2000 Å thickness on an oxidized aluminium foil in an Edwards sputter coater. Scanning electron microscopic (SEM) investigation of the evaporated films shows corrugations of submicrometer dimensions. Monolayers were prepared by following well-established procedures (2). One millimolar solution of MBT in absolute ethanol was exposed to freshly evaporated films overnight. After removal from the solution, films were washed with absolute ethanol. The films were mounted on the spectrometer immediately after removal from the solution. Raman spectra were measured with an FRA 106 FT-Raman accessory of a Bruker IFS 66V FT-IR spectrometer. An Nd-YAG laser (1064 nm) was used as the primary excitation source. Each spectrum was measured with 500 scans and acquisition took about 35 min. Variable temperature spectra were measured with a home-built heater and a programable temperature controller. X-ray photoelectron spectra were recorded with a VG ESCALAB Mk II spectrometer with unmonochromatized Mg$K\alpha$ radiation. In order to minimize beam-induced damage, the X-ray flux was kept low (electron power, 70 W). However, due to poor signal quality, the acquisition time had to be high, and we do not rule out beam-induced damage completely. No X-ray-induced desorption was observed in the experiment. *Ab initio* MO calculations were performed with the Gaussian 94 program (23) using the 6-31G* basis set (24, 25). C_s geometry was assumed for the calculations and all the molecular parameters were optimized in the calculation. Optimized molecular parameters were used as input for frequency calculations.

RESULTS AND DISCUSSION

Figure 1 shows the normal Raman (NR) spectrum of MBT and SER spectra of MBT monolayers on Au and Ag. The SER

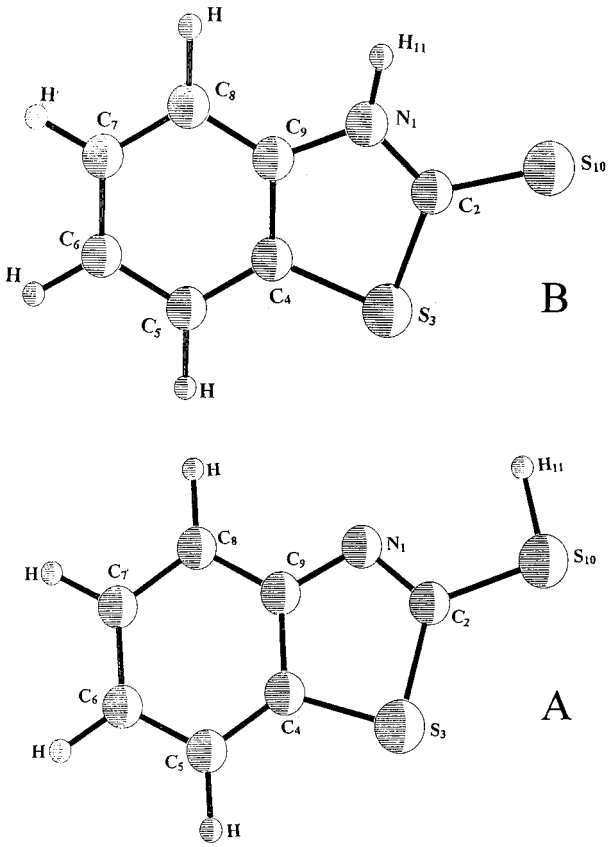

FIG. 2. The schematic molecular geometries of the (A) thiol and (B) thione forms of MBT. Molecular parameters from *ab initio* MO (HF/6-31G*) calculations are given in Table 2.

spectra are strikingly different from that of the solid, which indicates that only the adsorbed species are contributing to the intensity. The spectra of both the monolayers are different, which also reaffirms this point. In order to understand the spectrum, we performed *ab initio* MO calculations. MBT could exist in both thiol and thione forms and calculations were performed on both these forms. Figure 2 shows the schematic molecular geometries of the thiol and thione forms and Table 1 lists the optimized molecular parameters of these structures from calculations. The molecular geometries in these forms are substantially similar except for the N1-C2 and C2-S10 bond lengths. Concomitant changes are seen in the corresponding bond angles. Consequently, we see only minor changes in the computed Raman spectra of the two forms. Table 2 lists the scaled Raman frequencies of both the forms, as well as the experimental values for Ag and Au monolayers. In order to make these assignments, our spectra were compared with the IR and Raman spectra of related compounds, benzimidazole (26) and 2-amino-6-nitro benzothiazole (27).

All the frequencies are downshifted upon adsorption, as one would expect. Another feature is the broadening of all the peaks. Both aspects are characteristic of chemisorption. While the first effect is due to either dissociative chemisorption or metal–adsorbate charge transfer, the later is due to the presence of additional states at Fermi energy due to bonding and the presence of additional relaxation channels (28).

The striking feature that comes to immediate attention is the substantial changes in the C–H region of the monolayers (Fig. 1B). A normal Raman (NR) spectrum of MBT shows a weak peak at 2641 cm^{-1} attributed to the S–H stretch. This completely vanishes upon adsorption. The 3068-cm^{-1} band in the NR spectrum is attributed to the aromatic C–H stretches. The asymmetry of the peak shape is indicative of nondegenerate vibrations from the different C–H bonds. A number of other weak bands could be understood in terms of combinations. Whereas the C–H stretching mode in the monolayer is intense in Au, it is almost absent in Ag. In certain samples, we have, however, observed a weak feature in this region. In both the monolayers, the peak appears at almost the same value, red shifted by as much as 7 cm^{-1} in the monolayers from the spectrum of the solid.

The rather abrupt change in intensity is understandable from the published SERS selection rules (19–21), which enhance vibrations whose polarizability tensor components are perpendicular to the surfaces. If MBT were to adsorb such that its molecular plane is perpendicular to the surface, the component of the polarizability tensor of the aromatic C–H stretching modes normal to the surface will be larger in magnitude. But if the molecular plane is parallel to the surface, the polarizability tensor will have only a very weak component perpendicular to the surface. On the basis of this argument, adsorption geome-

TABLE 1

Optimized Molecular Parameters of Thiol and Thione Forms of MBT Obtained from HF/6-31G* Calculations[a] (See Fig. 2 for the Numbering Scheme.)

Parameters[b]	Thiol	Thione
R S3-S10	3.035	3.022
R N1-C2	1.265	1.341
R C2-S3	1.758	1.758
R S3-C4	1.750	1.761
R C4-C5	1.388	1.383
R C5-C6	1.380	1.385
R C6-C7	1.397	1.390
R C8-C9	1.392	1.384
R C9-N1	1.390	1.389
R C2-S10	1.763	1.650
A C2S3C4	88.0	91.8
A S3C2S10	119.1	125.1
A C2N1C9	110.2	117.6
A S3C2N1	116.8	108.9
A S10C2N1	124.1	125.9

[a] Distance is in Å units, and interatomic angle is in degrees. Torsional angles are not given since a C_s geometry is assumed.

[b] R refers to distances and A refers to angles.

TABLE 2

Observed and Scaled (Multiplied by 0.9) Theoretical Normal Raman Frequencies (in cm^{-1}) of 2-mercaptobenzothiazole Solid and SER Frequencies (in cm^{-1}) of MBT Monolayers on Au and Ag Surfaces

	Experimental values		From theoretical calculations				
Assignment[a]	IR	Raman	Thiol	Thione	Benzimidazole[b]	MBT on Au	MBT on Ag
νNH	—	—	—	3474	—	—	—
—	3112			—	—	—	—
νCH	3077	3068	3060	3059	3068	3061	3062
νCH	3040	3041	3051	—	—	—	—
νCH	—	—	3040	3040	—	—	—
νCH	2962	2962	3028	3032	—	—	—
—	2893	2890	—	—	—	—	—
—	2839	2837	—	—	—	—	—
νSH	—	2641	2647	—	—	—	—
νCC	1640	1601	1621	1624	1621	—	1586
νCC ip	1594	1582	1589	1608	1588	1579	1559
νCN	—	—	1557	—	—	—	—
—	—	—	—	—	1541		
νCC	1496	1495	—	1499	1496	—	—
νCC ip	1455	1457	1462	1476	1459	1451	1451
νCC	1432	1423	—	1431	1410	1408	1389
νCN	1319	1318	—	—	—	1313	1317
νCC	1282	1270	1276	1269	1302	1268	1276
νCC	1244	1252	—	1264	1247	1240	1242
δCH	—	—	1235	1224	—	—	—
δCH_{ip}	—	—	1213	1213	1202	—	—
δCH_{ip}	1148	1156	—	—	1157	—	—
δCH	1125	1130	1126	1124	1135	1131	1130
δCH	—	—	1102	1101	—	—	—
δCH ip	1077	1074	1076	1068	—	1100	1076
δCH ip	—	1050	—	—	—	1050	—
νCN	1034	1029	1035	1030	—	—	—
δCCC	1011	1013	—	—	1004	1010	1011
δCH	—	—	1006	1008	—	—	—
δCH	—	—	1005	1003	—	—	—
δCH	949	932	967	959	958	—	—
δCSH	—	—	909	—	—	—	—
δCH_{op}	867	865	880	874	885	865	868
δNH	—	—	—	843	—	—	—
δCH	—	—	840	—	835	—	—
δCH_{op}	750	756	771	762	769	753	758
δCH	—	—	735	723	—	—	—
νCS	—	704	693	694	—	706	713
νCS	667	662	639	650	—	673	—
νCS	603	606	592	—	—	—	601
δCNH	—	—	—	601	—	—	—
δCSH	568	—	583	—	—	—	—
δCNH	—	—	—	552	—	563	—
δCH	523	—	523	—	—	—	—
δNH	—	—	—	521	—	522	—
δCH	500	500	493	—	—	499	506
νCS	—	—	—	486	—	473	—
δCH	422	417	433	425	—	—	432
δCH	—	394	—	383	—	394	395
δCH	—	378	377	374	—	—	—
δCSH	—	—	358	—	—	—	—
δCH	—	289	294	281	—	267	310
δSH	—	213	209	204	—	204	205

[a] The designation ip refers to the in-plane vibrations, and op refers to the out-of-plane vibrations. The designation δ refers to bending vibrations, and ν to stretching vibrations.

[b] From Ref. (26). Assignments listed in this paper for the low frequency modes (below 769 cm^{-1}) are different from those in Ref. (26) and, therefore, are not listed.

tries of many of the organic systems have been evaluated (19, 21, 29, 30). An extension of the same argument would suggest that the molecular plane of MBT is perpendicular to the surface in Au but is flat on Ag. However, this would not completely define the adsorption geometry since there are two sulfur atoms and either or both of them could be involved in bonding. Analysis of the low-frequency region is necessary to resolve this issue.

The in-plane C–C stretching mode of MBT is observed at 1582 cm^{-1}. We observed substantial difference in intensity of these bands in both the monolayers. Whereas it is strong in Au, the intensity has decreased by an order of magnitude in Ag. This variation again could be interpreted in terms of SERS selection rules since this mode is along the molecular plane. The changes observed in the C═C as well as the C–C stretching regions are attributable to the same cause. In particular, note the substantial difference in intensity of the band at 1451 cm^{-1} in Au and Ag monolayers. Similar effects are also seen in the in plane C–H bending region. Whereas the band at 1050 cm^{-1} is of medium intensity in Au, it is completely absent in the Ag monolayer. SER spectra of adsorbed benzene and its derivatives studied by Gao and Weaver (31) and Gao *et al.* (32) also show this difference in intensities of in-plane and out-of-plane modes. In a flat adsorbate geometry, the in-plane modes decrease in intensity and the out-of-plane modes increase in intensity. This difference in the in-plane and out-of-plane modes has been elegantly used to conclude the preferential adsorbate geometry in a number of systems. Similar results are also available from the group of Kim *et al.* (33, 34).

Moreover, the difference in adsorption geometry of MBT on Ag and Au surfaces receives corraborative evidence from the voltametric characteristics of the two surfaces. One could expect this difference in adsorption geometry to result in an MBT monolayer that is less porous on Ag compared to that on Au (see below). This is substantiated by the observation (35) of ferro/ferricyanide redox kinetics becoming somewhat sluggish on Ag-MBT while remaining unhindered on Au-MBT.

The foregoing suggests that MBT is flat on Ag and perpendicular on Au. However, there can be several possible ways of surface binding. A qualitative understanding of the type of bonding is possible from the analysis of the C–S region. In the NR spectrum of MBT, this region shows three bands at 704, 662, and 606 cm^{-1}. The peak at 704 cm^{-1} is observed in both the surfaces and is assigned to one of the C–S modes of the heterocyclic ring system, and the shifts are not significant. The peak at 662 cm^{-1} occurs in Au but not in Ag. On the contrary, the 606 cm^{-1} peak is absent in Au but is present in Ag. A closer examination shows the emergence of other features in the 450 to 600 cm^{-1} region in the Au monolayer which also may have some C–S contribution. An analysis of this region requires support from theoretical calculations.

Theoretical calculations of the thiol geometry give three possible C–S vibrations. In increasing order of frequency, these vibrations are due to C4-S3, C2-S3, and C2-S10, respectively

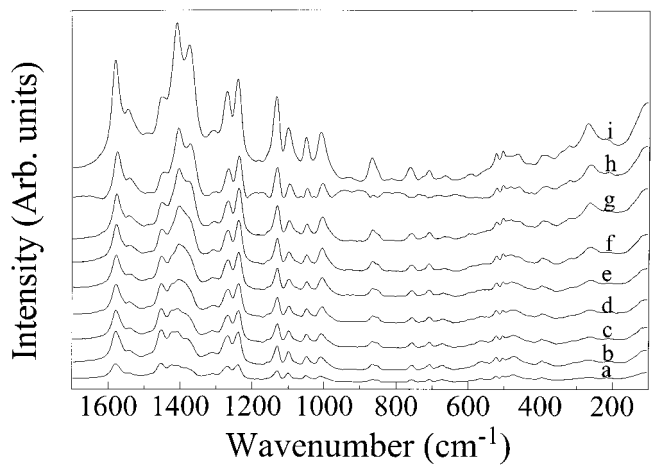

FIG. 3. Variable temperature SER spectra of MBT monolayer on Au. Parts (a), (b), (c), (d), (e), (f), (g), and (h) represent temperatures 298, 323, 348, 373, 398, 423, 448, and 473 K, respectively. Part (i) shows the spectrum upon cooling to room temperature. The C–H region is not shown where corresponding changes are observed.

(see Fig. 2 for the structure). The C2-S3 vibration is predominantly parallel to the molecular plane and this peak changes in intensity upon adsorption on Ag, which may be attributed to changes in adsorbate orientaion. However, unlike in the C–H and C–C regions, changes in the spectral features in the C–S region are not due to differences in orientation alone. In the thione geometry, the C–S vibrations occur at significantly different positions. The first two bands are due to C–S stretches involving C2-S3 and C2-S10, respectively, in decreasing order of frequency. The third frequency is due to C4-S3 vibration. An additional C–S stretch is predicted at 486 cm^{-1} for the thione form. The emergence of a new band around the predicted frequency region in the Au monolayer and the complete disappearance of the band at 606 cm^{-1} may be attributed to the thione structure on Au. Supportive evidence for this argument comes from the emergence of two new peaks at 563 and 522 cm^{-1} attributed to C–N–H bend and N–H deformation, respectively. The N–H stretch predicted to occur at 3474 cm^{-1} is, however, not observed in the spectrum due to instrumental limitations.

In Fig. 3 we present the variable temperature SERS data of an MBT monolayer on Au. The most remarkable aspect of these data is the stability of the monolayer even up to a temperature of 473 K, much higher than the desorption temperature of alkanethiol monolayers (7). The C–S region does not exhibit any change with temperature, suggesting the absence of structural changes in the monolayer. The peak intensity of almost all features increases substantially and is particularly noticeable in the C═C region. The spectrum obtained upon cooling the monolayer to room temperature is markedly different and suggests that an irreversible change has occurred. A closer examination shows that the frequencies remain at the original values but the intensities of the peaks have increased.

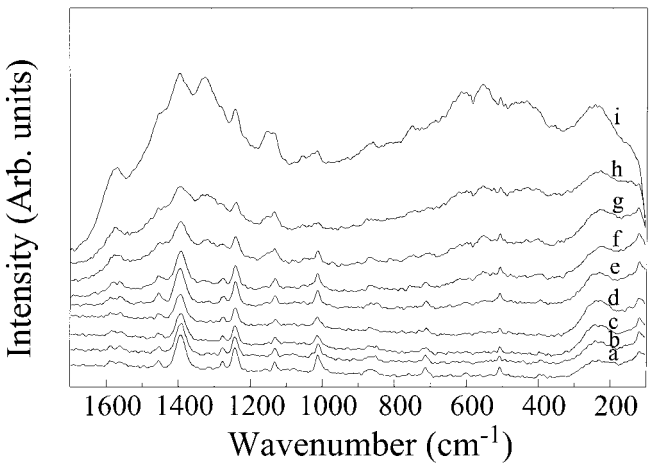

FIG. 4. Variable temperature SER spectra of MBT monolayer on Ag. Parts (a), (b), (c), (d), (e), (f), (g), and (h) represent temperatures 298, 323, 348, 373, 398, 423, 448, and 473 K, respectively. Part (i) shows the spectrum after cooling to room temperature.

A slightly similar effect is seen in Ag (see below). Corresponding changes are observed in the C–H region also (not shown). We attribute this to the annealing of the monolayers and the aggregation of gold islands at the surface leading to a more extended and ordered monolayer. The coalescence of Au islands upon annealing has been observed earlier in a scanning tunneling microscopic (STM) investigation (36). The annealing appears to be driven by the presence of the monolayer. It may be noted that capped gold clusters organize to form a hexagonal lattice, due to the presence of the organization of the capping molecules (37, 38). A similar effect seems to be driving the gold islands to coalesce.

The temperature dependence of the SERS spectrum of the Ag monolayer is presented in Fig. 4. Similar to the Au case, a denser monolayer is observed upon cooling. However, unlike in the case of Au, the peaks get substantially broadened. We attribute this to incomplete removal of strains in the monolayer and the possible occurrence of defects at the grain boundaries. Coalescence of islands has occurred, leading to the substantial increase in the Raman intensity. Apart from the general increase in the intensity of all bands, certain new bands are observed, particularly at 1313, 1050, and 550 cm^{-1}, which could be attributed to the coexistence of other possible adsorbate geometries at the surface. Since most of the features remain at the original positions, a uniform structural change is not suggested.

It is important to note that the variable temperature measurements of the monolayers do not manifest significant changes (compared to other systems we have investigated earlier), although adsorption geometry is different in both cases. In an earlier investigation we have shown that different adsorption geometries lead to different temperature-dependent Raman spectra (8). The absence of such a variation can be due to strong surface binding and/or dense self assembly. This may be taken to suggest that, irrespective of the thione or thiol structure, surface binding is strong.

Having established the surface geometry, it is important to inquire why such a difference should occur. In both thiol and thione geometries, the S–S distances are similar, namely 3.035 and 3.022 Å, respectively (see Fig. 2 and Table 1). The preferred binding sites for alkanethiols on Au(111) are the threefold hollow sites (39). The near-neighbor threefold hollow site distances on Au(111) and Ag(111) are 2.885 and 2.890 Å, respectively. Therefore, differences in the S–S distances and the lattice constants are not the reason for the observed difference in adsorption geometry. The only reason we could attribute this to is the preferential π bonding on Ag and the absence of it on Au. The presence of a π orbital on nitrogen would also support a ring-surface π interaction, and therefore such an adsorbate structure is favorable for Ag.

In order to understand the nature of the chemical state of elements at the surface and to explore the changes that occur to the substrate atoms upon adsorption, we performed XPS investigations on the monolayers. The Au4$f_{7/2}$ occurs as a single peak at 84.0 eV binding energy (BE), suggesting the absence of chemical changes of the bulk substrate atoms. The Ag3$d_{5/2}$ occurs at 368.2 eV, which again indicates absence of changes in the bulk of the substrate. The S2p regions of both the monolayers are shown in Fig. 5. S2p occurs as a single peak at 164.0 eV BE higher than the thiolate BE normally seen for alkanethiol monolayers. The $Au^{+}S^{-}$ thiolate binding leads to a S2p structure at 162 eV BE (40). The increase in BE is

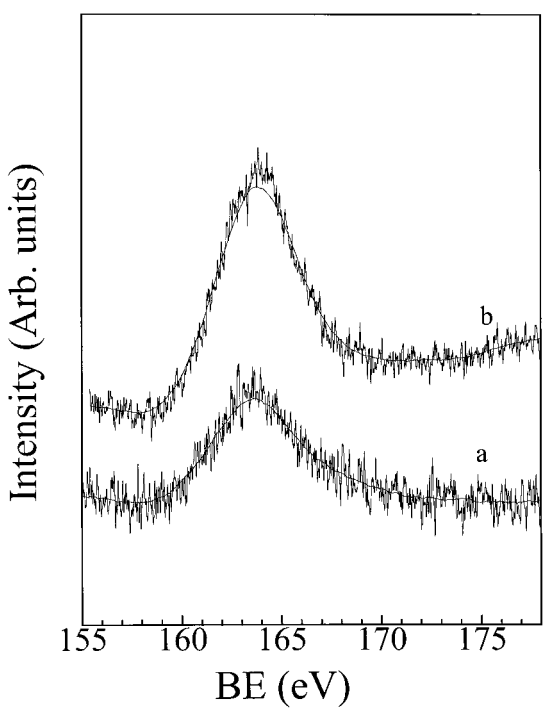

FIG. 5. X-ray photoelectron spectra of MBT monolayers on Au (a) and Ag (b) in the S2p region.

attributed to the covalent nature of the binding. Although dissociative chemisorption has occurred in Ag, leading to the thiolate structure, the charge appears to be heavily delocalized, as one would expect from the structure. It is seen that two separate features are not observed corresponding to the two sulfurs. Both thiol and thione forms in the solid state would show peaks in the range 163–164 eV BE, and two distinct features are not expected at the instrumental resolution (1eV).

A general observation is that the intensity of the peaks is lower on Au than on Ag. This may be seen from the extent of noise present in the spectrum. This is the case with other regions also. Seemingly the surface coverage is poor on Au (an aspect supported by electrochemical studies, see above), which could be the reason for the large intensity enhancement of peaks in SERS upon heating. However, the difference in intensity could also be attributed to the difference in adsorbate geometry on these surfaces as well. Since the molecules are adsorbed perpendicular to the surface on Au, the thickness of the monolayer is larger than on Ag. Consequently, the inelastic scattering of S2*p* photoelectrons will be greater on Au contributing to the lower intensity. However, the extent of intensity reduction is not fully explainable from this cause alone and both factors appear to be responsible.

The C1*s* and N1*s* regions of Au and Ag monolayers are shown in Figs. 6A and 6B, respectively. C1*s* appears as a single peak at 285.0 eV BE, characteristic of adsorbed hydrocarbons and alkane thiolate SAMs (6). The N1*s* feature in the Au monolayer appears at 398.8 eV and in Ag it is at 400.2 eV BE, characteristic of adsorbed amines and other similar systems (41). The small difference in N1*s* binding energies can be understood in terms of X-ray-induced chemical changes. The general observation on intensities made earlier is valid here too.

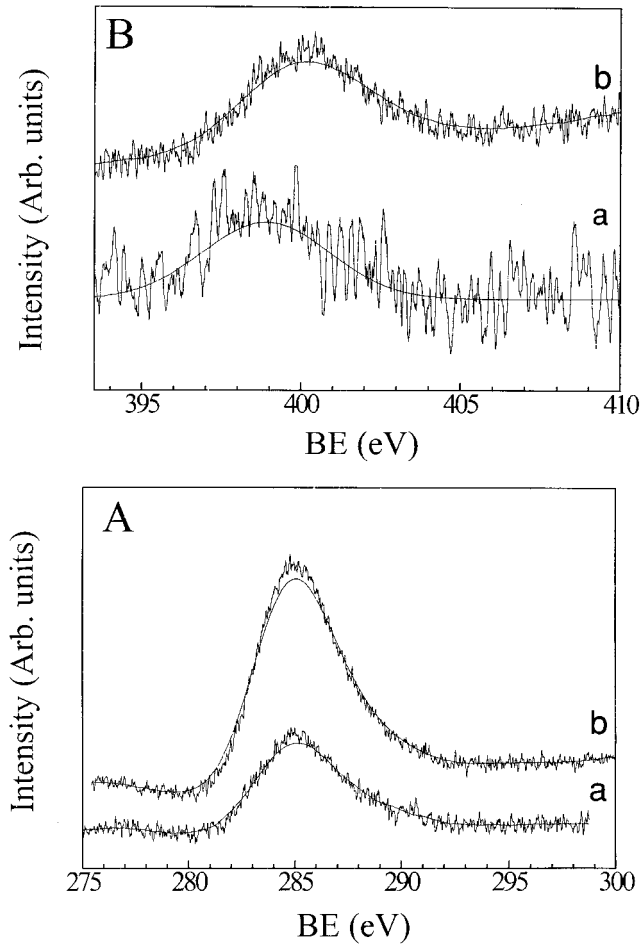

FIG. 6. X-ray photoelectron spectra in the C1*s* (A) and N1*s* (B) regions of Au (a) and Ag (b) monolayers. Due to poor signal quality, the N1*s* region of the Au monolayer is more noisy.

CONCLUSION

We have demonstrated the difference in adsorption geometries of MBT monolayers on Au and Ag. An analysis of the C–S region with the help of *ab initio* MO calculations suggests that MBT adsorbs in the thione form on Au and in the thiol form on Ag. We conclude that the molecular plane of MBT is perpendicular to the surface on Au and parallel to the surface on Ag, and this may be due to the preferential π bonding on Ag, which is absent on Au. The most significant feature of MBT monolayers is their stability up to a temperature of 473 K. The enhancement of peak intensities with temperature is explained as being due to the annealing of the monolayers and the subsequent formation of well-ordered and extended molecular assembly as a result of the aggregation of metal islands. We have also shown the covalent nature of surface binding from the S2*p* XPS data.

ACKNOWLEDGMENTS

T.P. thanks the Department of Science and Technology, Government of India, Rajiv Gandhi Foundation, and Jawaharlal Nehru Centre for Advanced Scientific Research for funding this research program on SAMs. N.S. thanks the Council of Scientific and Industrial Research, New Delhi, for the award of a research fellowship.

REFERENCES

1. Whitesides, G. M., Ferguson, G. S., Allara, D. L., Scherson, D., Speaker, I., and Ulman, A., *Surf. Chem.* **3,** 49 (1993).
2. Ulman, A., *in* "An Introduction to Ultrathin Organic Films: From Langmuir Blodgett to Self Assembly." Academic Press, New York, 1991.
3. Cooks, R. G., Ast, T., Pradeep, T., and Wysocki, V. H., *Acc. Chem. Res.* **27,** 316 (1994). [An overview of reactions of ions at molecular surfaces can be found here]
4. Bindu, V., Dorothy, A., and Pradeep , T., *Int. J. Mass Spectrom. Ion Processes* **155,** 69 (1996).
5. Bindu, V., Venkataramanan, M., and Pradeep, T., *Mol. Phys.,* in press.
6. Bindu, V., and Pradeep, T., *Vacuum* **49,** 63 (1998).
7. Sandhyarani, N., and Pradeep, T., *Vacuum* **49,** 279 (1998).

8. Murty, K. V. G. K., Venkataramanan, M., and Pradeep, T., *Langmuir* **14,** 4446 (1998).
9. Lipkowski, J., Stolberg, L., *in* "Adsorption of Molecules at Metal Electrodes" (J. Lipkowski, and P. N. Ross, Eds.). VCH, New York, 1992.
10. Hatta, A., Chiba, Y., and Suetaka, W., *Surf. Sci.* **158,** 616 (1985).
11. Bharathi, S., Yegnaraman, V., and Prabhakara Rao, G., *Langmuir* **9,** 1614 (1993).
12. Berchmans, S., Yegnaraman, V., and Prabhakara Rao, G., *Proc. Indian Acad. Sci. Chem. Sci.* **109,** 277 (1997).
13. Liu, C., Zhang, Z., and Ren, X., *Wuli Huaxue Xuebao* **9,** 533 (1993).
14. Liu, C., Zhang, Z., and Ren, X., *Chin. Chem. Lett.* **3,** 539 (1992).
15. Ohsawa, M., and Suetaka, W., *J. Electron Spectrosc. Relat. Phenom.* **30,** 221 (1983).
16. Gi, Xue, and Yun, Lu, *Langmuir* **10,** 967 (1994).
17. Gi, Xue, and Zhang, J., *J. Appl. Spectrosc.* **45,** 760 (1991).
18. Brown, N. M. D., Meenan, B. J., and Taggart, G. M., *Spectrochim. Acta* **47A,** 387 (1991).
19. Moskovits, M., and Suh, J. S., *J. Phys. Chem.* **88,** 5526 (1984).
20. Moskovits, M., and Suh, J. S., *J. Phys. Chem.* **92,** 6327 (1988).
21. Creighton, J. A., *Surf. Sci.* **124,** 204 (1983).
22. Sandhyarani, N., Murty, K. V. G. K., and Pradeep, T., *J. Raman. Spectrosc.* **29,** 359 (1998).
23. Frisch, M. J., Trucks, G. W., Schlegel, H. B., Gill, P. M. W., Johnson, B. G., Robb, M. A., Cheeseman, J. R., Keith, T. A., Peterson, G. A., Montgomery, J. A., Raghavachari, K., Al-laham, M. A., Zakrzewski, V. G., Ortiz, J. V., Foresman, J. B., Cioslowski, J., Stefanov, B. B., Nanayakkara, A., Challacombe, M., Peng, C. Y., Ayala, P. Y., Chen, W., Wong, M. W., Andres, J. L., Replogle, E. S., Gomperts, R., Martin, R. L., Fox, D. J., Binkley, J. S., Defrees, D. J., Baker, J., Stewart, J. P., Head-gordaon, M., Gonzalez, C., and Pople, J. A., "Gaussian 94." Gaussian, Inc., Pittsburgh, PA, 1995.
24. Dill, J. D., and Pople, J. A., *J. Chem. Phys.* **62,** 2921 (1975).
25. Binkley, J. S., and Pople, J. A., *J. Chem. Phys.* **66,** 879 (1977).
26. Mohan, S., Sundaraganesan, N., and Mink, J., *Spectrochim. Acta* **47A,** 1111 (1991).
27. Mohan, S., Prabakaran, A. R., and Payami, F., *J. Raman Spectrosc.* **20,** 455 (1989).
28. Otto, A., Mrozek, I., Grabhorn, H., and Akemann, W., *J. Phys. Condensed Matter* **4,** 1143 (1992).
29. Pagannone, M., Formari, B., and Mattei, G., *Spectrochim. Acta* **43A,** 621 (1987).
30. Suh, J. S., Dilella, D. P., and Moskovits, M., *J. Phys. Chem.* **87,** 1540 (1983).
31. Gao, P., and Weaver, M. J., *J. Phys. Chem.* **89,** 5040 (1985).
32. Gao, X., Davies, J. P., and Weaver, M. J., *J. Phys. Chem.* **94,** 6858 (1990).
33. Cho, S. H., Han, H. S., Jang, D-J., Kim, K., and Kim, M. S., *J. Phys. Chem.* **99,** 10594 (1995).
34. Lee, T. G., Kim, K., and Kim, M. S., *J. Phys. Chem.* **95,** 9950 (1991).
35. Berchmans, S., and Yegnaraman, V., unpublished results.
36. Dishner, M. H., Hemminger, J. H., and Feher, F. J., *Langmuir* **13,** 4788 (1997).
37. Whitten, R. L., Khoury, J. T., Alvarez, M. M., Murthy, S., Vezmar, I., Wang, Z. Z., Stephens, C. L., Cleveland, W. D., Luedtke, W. D., and Landmans, U., *Adv. Matter* **8,** 428 (1996).
38. Vijaya Sarathy, K., Raina, G., Yadav, R. T., Kulkarni, G. U., and Rao, C. N. R., *J. Phys. Chem. B* **101,** 9876 (1997).
39. Sellers, H., Ulman, A., Shnidman, Y., and Eilers, J. E., *J. Am. Chem. Soc.* **115,** 9389 (1993).
40. Bain, C. D., Troughton, E. B., Tao, Y. T., Eoall, J., Whitesides, G. M., and Nuzzo, R. G., *J. Am. Chem. Soc.* **111,** 321 (1989).
41. Briggs, D., and Seah, M. D., *in* "Practical Surface Analysis by Auger and X-Ray Photoelectron Spectroscopy." Wiley, Chichester, 1984.